

# MORN: Metacognitive Object-Goal Regulation for Resource-Rational Long-Horizon Navigation

Xi Lin<sup>1,3,\*</sup>, Jiayi Li<sup>3,\*</sup>, Kangyi Wu<sup>2,3</sup>, Jiaqiao Tang<sup>3</sup>, Qingrong He<sup>3</sup>, and Lin Zhao<sup>3,†</sup>

**Abstract**—Robots deployed in unstructured human environments must frequently execute long-horizon missions—such as “find the mug, then the chair, then the printer”—under strict operational constraints. While contemporary zero-shot Object Navigation (ObjectNav) agents leverage Vision-Language Models (VLMs) to effectively localize semantic targets, they operate as purely reactive systems that inherently lack global resource awareness. Consequently, these agents inadvertently exhaust critical budgets (time, battery) on infeasible subgoals due to partial observability, failing to balance local exploration with global mission viability. To bridge this gap by injecting resource-rationality into the navigation loop, we present MORN (Metacognitive Object-goal Regulation Navigation), an executive architecture inspired by Dual-Process Theory in cognitive science. MORN augments frozen navigation backbones with a “System 2” meta-controller that continuously monitors the “System 1” locomotor. By formalizing three neuro-cognitive states—Potentiality Index, Persistence Gating, and Evidence Accumulation—MORN dynamically regulates the mission schedule based on online estimates of progress velocity and perceptual uncertainty. This mechanism effectively neutralizes the Sunk Cost Fallacy, enabling agents to abort “zombie goals” early and decisively commit to achievable ones. Extensive experiments on the HM3D dataset demonstrate that MORN improves Goal Completion Rate (CR) from 0.23 to 0.30 and reduces Wasted Step Fraction (WSF) from 0.90 to 0.70, establishing that in resource-constrained autonomy, the metacognitive awareness of global resources is as critical as the reactive ability to navigate.

## I. INTRODUCTION

The pursuit of embodied intelligence has undergone a paradigm shift with the advent of Vision-Language Models (VLMs) and open-vocabulary perception. Agents can now navigate to semantic targets in unseen environments without task-specific training, achieving impressive zero-shot generalization in single-goal ObjectNav benchmarks.

In multi-goal navigation, every step spent on one goal depletes the resources available for others. This introduces a resource zero-sum constraint, where traditional greedy approaches, while effective in single-goal tasks, fail catastrophically in multi-goal settings. The agent must continuously decide whether to persist on the current goal (exploiting accumulated search effort) or abandon it to switch to a more promising target (exploration at the executive level)—a



Fig. 1. **Obsessive vs. Metacognitive Behavior.** Left: Standard ObjectNav agents fall into the “Sunk Cost Trap,” exhausting the global budget on a single infeasible goal. Right: MORN enforces “Resource Rationality” by strategically aborting “zombie goals” early. This preserves critical resources (time/battery) for subsequent solvable targets, maximizing overall mission utility.

decision that requires estimating the expected value of future goals under uncertainty.

Compared to single-goal ObjectNav, multi-goal episodes introduce three structural constraints that cannot be removed by a stronger low-level navigator alone. First, budget coupling means every step spent on one goal is a step not available for the rest; hence a locally reasonable search can globally collapse the mission. Second, information incompleteness makes “not found yet” indistinguishable from “infeasible from here,” especially in large indoor layouts where open-vocabulary evidence is sparse and intermittent. Third, termination is high-risk: declaring success too early causes irreversible downstream errors, while persisting too long creates “zombie goals” that monopolize the episode. In practice, these failure modes are directly visible as a high wasted-step fraction (WSF) with low completion rate (CR).

Current zero-shot ObjectNav agents are architecturally designed as pure “System 1” reactive systems—fast, persistent, and stimulus-driven. Lacking a “System 2” metacognitive layer, they exhibit a pathology we term obsessive persistence: when confronted with a difficult or infeasible target, they fall into the Sunk Cost Fallacy, continuing to invest budget solely because they have already invested it. Empirical analysis reveals that baseline systems waste up to 90% of their operational budget on goals that are never completed.

To address this architectural gap, we introduce MORN (Metacognitive Object-goal Regulation Navigation), a training-free executive layer that instills resource rationality into frozen VLM-based navigation backbones. MORN operates as the “System 2” deliberative supervisor: it does

\* Equal contribution. † Corresponding author

<sup>1</sup> Xi Lin is with the LCSR Lab, Johns Hopkins University (xilin03@outlook.com).

<sup>2</sup> Kangyi Wu is with Xi’an Jiaotong University (wukangyi747600@stu.xjtu.edu.cn).

<sup>3</sup> The authors are with JD Explore Academy, Beijing, China. (zhaolins@foxmail.com).

not alter the low-level locomotion policy but regulates it by continuously monitoring introspective signals—progress velocity, perceptual evidence strength, and temporal stability—to dynamically control persistence, switching, abandonment, and commitment decisions.

Our contributions are summarized as follows:

- **Dual-Process Mechanism:** We propose a decoupled architecture that installs a “System 2” regulator atop any frozen “System 1” navigator. This allows for plug-and-play budget awareness without retraining the underlying policy.
- **Neuro-Cognitive State Space:** We bridge the gap between abstract resource rationality and robotic control by formalizing interpretable meta-states—Potentiality ( $\Pi_t$ ), Persistence ( $\Gamma_t$ ), and Evidence ( $\Sigma_t$ ). These states transform raw VLM signals into actionable executive decisions.
- **Resource-Constrained Protocol:** We construct a rigorous Multi-Goal Benchmark on HM3D that explicitly penalizes inefficient search. Experiments show that MORN reduces Wasted Step Fraction (WSF) by 20% relative to baselines, establishing that in long-horizon missions, knowing *when to stop* is as critical as knowing *how to move*.

## II. RELATED WORK

### A. Zero-Shot and VLM-Guided Navigation

The evolution of ObjectNav has moved from end-to-end Reinforcement Learning (RL) towards modular, zero-shot systems [29]. Early works relied on massive RL training with category-specific rewards, limiting generalization. Recent approaches utilize VLMs (e.g., CLIP [23], BLIP-2 [24], GLIP [25]) to construct semantic maps or frontier potentials [33]. For instance, VLFM [1] builds a semantic value map to guide exploration, while ZSON [2] leverages multimodal goal embeddings. However, these methods operate under a “single-goal” assumption. When applied to multi-goal sequences, they default to a greedy “run-until-completion” strategy. Recent training-free systems [3], [4], [5] combine geometric exploration with open-vocabulary scoring but treat termination as a local decision based on instantaneous evidence. Complementary scene graph-based approaches [6], [7], [8] enhance spatial reasoning but similarly lack executive resource management. MORN is complementary: we assume a fixed backbone and focus on executive regulation—deciding when to persist, switch, or stop under a shared global budget.

### B. Multi-Goal Task Planning

Multi-goal navigation has historically been treated as a geometric path planning problem, akin to the Traveling Salesperson Problem (TSP) [20] or coverage planning [34]. These formulations assume known goal locations and focus on minimizing travel distance. In contrast, ObjectNav involves discovering goal locations online under partial observability. Related work includes image-goal navigation [14], [12], where visual goals guide exploration, and recent surveys [18]

categorize knowledge integration strategies. Heuristics like “Greedy Nearest Neighbor” (ReactiveOrder) attempt to adapt TSP logic to unknown environments but fail to account for goal uncertainty. While multi-goal navigation has been studied in task planning [17], many formulations assume weak coupling between goals or explicit reward signals. In our setting, the dominant failure is not route suboptimality but time misallocation under uncertainty. Our benchmark protocol isolates this difficulty by composing 2- and 3-goal episodes while keeping the underlying single-goal navigator unchanged.

### C. Cognitive Architectures and Resource Rationality

Metacognition refers to an agent’s ability to monitor and regulate its own cognitive processes [19]. In robotics, introspective frameworks have been explored for failure prediction and anomaly detection. Our work draws specifically from **Dual-Process Theory** [19] and **Resource Rational Analysis**, which treat computation and action as costly resources to be optimized. Unlike “black-box” meta-controllers trained via end-to-end RL [21], [22] or LLM-based planners [38], [39], MORN operationalizes these abstract concepts into transparent signals. We explicitly map the psychological constructs of *affordance*, *inhibitory control*, and *evidence accumulation* into mathematical states ( $\Pi_t$ ,  $\Gamma_t$ ,  $\Sigma_t$ ) derived from navigation telemetry. This provides a lightweight, interpretable layer that bridges the gap between cognitive science principles and practical robotic control (Table I).

## III. METHOD: MORN

### A. Theoretical Formulation: Budget-Constrained Utility

We formalize the Multi-Goal ObjectNav task as a Partially Observable Semi-Markov Decision Process with a finite budget. Let the mission be defined by a tuple  $\mathcal{T} = \langle \mathcal{G}, B_{max}, \mathcal{E} \rangle$ , where  $\mathcal{G} = \{g_1, \dots, g_K\}$  is the set of semantic goals and  $B_{max}$  is the total step budget.

The agent’s objective is not merely to find goals, but to maximize the total mission utility  $J$ :

$$J = \sum_{k=1}^K R(g_k) \cdot \mathbb{I}(\text{success}(g_k)) - \lambda \cdot \text{Cost}_{total}, \quad (1)$$

subject to  $\text{Cost}_{total} \leq B_{max}$ . Here,  $R(g_k)$  is the reward for goal  $g_k$ , and  $\text{Cost}_{total}$  is the total cost. Crucially, the budget constraint creates a dependency:

$$P(\text{success}(g_j) \mid \text{persist}(g_i)) \propto B_{max} - \text{Cost}(g_i). \quad (2)$$

Persisting on goal  $g_i$  directly reduces the probability of success for subsequent goal  $g_j$  by depleting the shared resource  $B_{max}$ . The optimal policy must therefore estimate the expected future value of switching versus persisting.

### B. The Dual-Process Architecture

MORN implements a hierarchical control structure:

**System 1 (Navigation Backbone):** A frozen, reactive policy  $\pi_{nav}(o_t, g)$  that maps observations to primitive actions (e.g., MoveForward). It handles the “How” of navigation.

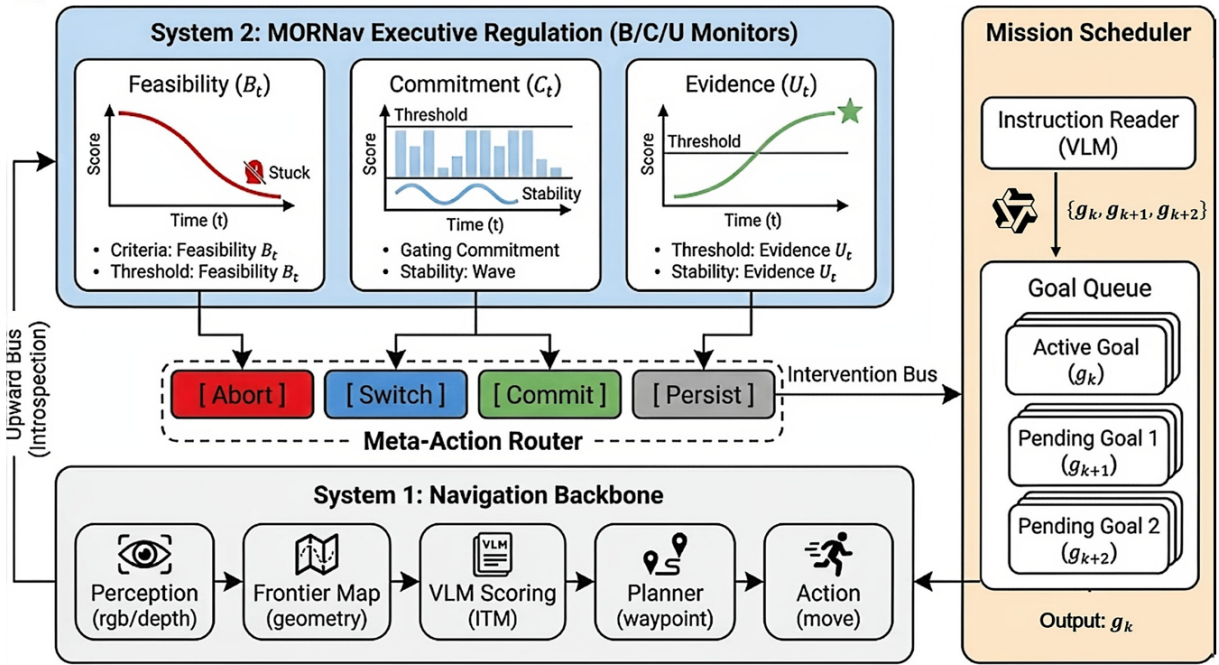


Fig. 2. **MORN Dual-Process Architecture.** The framework decouples navigation into two distinct systems. System 1 (Bottom) is a reactive navigation backbone that handles locomotion and perception. System 2 (Top) acts as the metacognitive executive. It monitors the backbone via the Upward Bus, computing three neuro-cognitive states (Feasibility  $\Pi_t$ , Commitment  $\Gamma_t$ , Evidence  $\Sigma_t$ ). Based on these states, the Meta-Action Router issues high-level interventions (PERSIST, SWITCH, ABORT, COMMIT) via the Intervention Bus to regulate the mission schedule without retraining the low-level policy.

**System 2 (MORN Executive):** A deliberative meta-policy  $\pi_{\text{meta}}(h_t)$  that maps the introspective history  $h_t$  to high-level interventions  $m_t \in \{\text{PERSIST, SWITCH, ABORT, COMMIT}\}$ . It handles the “Whether” of navigation as follows:

$$a_t \sim \pi_{\text{nav}}(o_t, g_{k_t}), \quad m_t = \pi_{\text{meta}}(h_t). \quad (3)$$

### C. Introspective Signal Processing

*Design rationale (signals).* MORN is built around the minimum set of signals that jointly explain the dominant multi-goal failure modes. Progress captures whether the agent is actually improving reachability rather than wandering. Evidence strength (ITM confidence) indicates potential target presence but is unreliable when used alone. Evidence stability distinguishes transient spikes from persistent confirmation, which is critical because premature commitment is an irreversible error in multi-goal episodes. Finally, sunk cost quantifies how much budget has already been invested into a goal, enabling explicit control of diminishing returns and preventing “obsessive persistence.”

*Design rationale (state  $\rightarrow$  mode).* The meta-states are not additional learned modules; they are a compact executive summary of the above signals. Potentiality (or Feasibility) answers “is this goal still promising?”, Persistence Gating (or Commitment) answers “is continued investment justified given diminishing returns?”, and Evidence Accumulation (or Sufficiency) answers “is it safe to terminate with success?”. The four executive modes (PERSIST/SWITCH/ABORT/COMMIT) then provide an explicit interface that can be audited and tuned, rather than entangling long-horizon scheduling with low-level action selection.

MORN extracts three key signals from the backbone’s **Progress Velocity** ( $v_t^{\text{nav}}$ ). We use progress velocity as the rate of geodesic distance reduction or frontier coverage. In simulation, we utilize ground-truth geodesic distance to rigorously test the upper bound of regulation; in real-world deployment, this is approximated by frontier exploration rates. **Evidence Strength** ( $s_t$ ). Evidence strength is the raw confidence score from the VLM perception head (e.g., CLIP [23] cosine similarity or detection scores [26], [27]). **Evidence Stability** ( $s_t^{\text{stab}}$ ). To filter perceptual noise, we compute temporal stability using an exponential moving average (EMA) and variance windowing. The smoothed score and variance are computed as:

$$\bar{s}_t = \alpha \bar{s}_{t-1} + (1 - \alpha) s_t, \quad \text{Var}_t(s) = \frac{1}{W} \sum_{i=t-W+1}^t (s_i - \bar{s}_t)^2, \quad (4)$$

where  $\alpha$  is the EMA decay factor and  $W$  is the rolling window size (set to  $W = 5$  frames, see Table III). The stability score is then derived by inverting the normalized variance:

$$s_t^{\text{stab}} = 1 - \text{CLIP}\left(\frac{\text{Var}_t(s)}{\sigma_s + \epsilon}, 0, 1\right), \quad (5)$$

where  $\text{CLIP}(x, a, b) = \max(a, \min(x, b))$  bounds the input to the range  $[a, b]$ . The CLIP operation serves a critical role: it limits the normalized variance ratio to  $[0, 1]$ , preventing numerical instability when variance spikes occur. By capping extreme values, CLIP ensures that the stability score reliably distinguishes transient noise (high variance) from persistent confirmation (low variance). Without this bounding, instantaneous perceptual spikes—common in zero-shot VLM outputs—

TABLE I  
NEURO-COGNITIVE MAPPING: FROM CONCEPT TO EXECUTION

Meta-Action	Cognitive Interpretation	Operational Role in MORN
PERSIST	Goal Maintenance	Default state. Continue search when progress $\Pi_t$ is stable.
SWITCH	Cognitive Flexibility	Re-allocate attention when inertia $\Gamma_t$ outweighs marginal information gain.
ABORT	Inhibitory Control	Inhibit "zombie goals" when feasibility $\Pi_t$ drops below critical threshold.
COMMIT	Decision Thresholding	Terminate only when evidence $\Sigma_t$ accumulates beyond noise levels.

could dominate the stability estimate and trigger premature commitment. Here,  $\sigma_s$  is a normalization constant calibrated to typical ITM score variance, and  $\varepsilon$  is a small constant ( $10^{-6}$ ) to prevent division by zero.

#### D. Neuro-Cognitive State Space

We transform raw signals into three high-level states:

1) *Potentiality Index* ( $\Pi_t$ ): “Affordance of Success”: This state estimates the environment’s current “affordance” for the active goal. It answers: *Is the search strategy yielding tangible progress?*

$$z_t^\Pi = w_v \cdot v_t^{\text{nav}} + w_s \cdot s_t + w_{\text{stab}} \cdot s_t^{\text{stab}}, \quad \Pi_t = \sigma(z_t^\Pi), \quad (6)$$

where  $z_t^\Pi$  is the weighted linear combination of introspective signals,  $w_v$ ,  $w_s$ , and  $w_{\text{stab}}$  are scalar weight coefficients that balance the relative importance of progress velocity, evidence strength, and evidence stability respectively, and  $\sigma(\cdot)$  is the sigmoid activation function that maps the weighted sum to  $[0, 1]$ . In our implementation, we set  $w_v = 0.4$ ,  $w_s = 0.3$ , and  $w_{\text{stab}} = 0.3$  based on preliminary tuning. A consistently low  $\Pi_t$  indicates the agent is exploring “dead zones” (low information gain), triggering an ABORT to prevent further waste.

2) *Persistence Gating* ( $\Gamma_t$ ): “Inertia vs. Gain”: This state acts as a gatekeeper against the Sunk Cost Fallacy. It models the tension between information gain and investment inertia.

We define investment inertia  $\mathcal{I}(c_t) = c_t/B_{\text{sub}}$  as the fraction of the subgoal budget already consumed. We define information gain  $g_t^{\text{info}} = \text{Var}_{t-W}(s) - \text{Var}_t(s)$  as the reduction in evidence variance over the rolling window, indicating whether new observations are resolving uncertainty.

$$z_t^\Gamma = u_g \cdot g_t^{\text{info}} - u_i \cdot \mathcal{I}(c_t) + u_v \cdot v_t^{\text{nav}}, \quad \Gamma_t = \sigma(z_t^\Gamma), \quad (7)$$

where  $u_g$ ,  $u_i$ , and  $u_v$  are weight coefficients for information gain, inertia penalty, and navigation velocity, respectively. In our implementation,  $u_g = 0.5$ ,  $u_i = 0.3$ , and  $u_v = 0.2$ . If  $\Gamma_t$  decays below a threshold  $\tau_\Gamma$  (also denoted  $\tau_S$  in Table III), the gate closes, triggering a SWITCH to reallocate the remaining budget to a fresh goal.

3) *Evidence Accumulation* ( $\Sigma_t$ ): “Drift-Diffusion Decision”: To ensure robust termination, we model the completion decision as an Evidence Accumulation process.

$$\Sigma_t = w_e \cdot s_t + w_{\text{stab}} \cdot s_t^{\text{stab}} + w_{\text{prox}} \cdot \text{Prox}(d_t), \quad (8)$$

where  $w_e$ ,  $w_{\text{stab}}$ , and  $w_{\text{prox}}$  are weight coefficients for evidence strength, stability, and spatial proximity, and  $\text{Prox}(d_t) = \exp(-d_t/\lambda_{\text{prox}})$  is a proximity kernel that decays

#### Algorithm 1 MORN metacognitive controller (per-step).

---

```

1: Input: goal set  $\mathcal{G}$ , backend  $\pi_{\text{nav}}$ , thresholds  $(\tau_A, \tau_S, \tau_C)$ , window  $W$ , grace period  $T_g$ , caps  $(B_{\text{max}}, B_{\text{sub}})$ 
2: Initialize active goal index  $k \leftarrow 1$ ; per-goal steps  $c \leftarrow 0$ ; ITM buffer  $\mathcal{S} \leftarrow \emptyset$ ; smoothed score  $\bar{s} \leftarrow 0$ 
3: for  $t = 1$  to  $B_{\text{max}}$  do
4:   Observe  $o_t$ ; execute  $a_t \leftarrow \pi_{\text{nav}}(o_t, g_k)$  and log signals  $(d_t, s_t)$ 
5:   Update rolling window:  $\mathcal{S} \leftarrow \text{last-}W$  of  $\mathcal{S} \cup \{s_t\}$ ; update  $\bar{s}$ ; compute  $\text{Var}_t(s)$  and stability  $s_t^{\text{stab}}$ 
6:   Compute meta-states  $(\Pi_t, \Gamma_t, \Sigma_t)$  from progress, evidence strength, stability, and sunk cost  $c$ 
7:   if  $t \geq T_g$  and  $\Pi_t < \tau_A$  then
8:     ABORT: mark  $g_k$  failed;  $k \leftarrow \text{SelectNext}(\mathcal{G}_{\text{rem}})$ 
9:     Reset:  $c \leftarrow 0$ ,  $\mathcal{S} \leftarrow \emptyset$ ,  $\bar{s} \leftarrow 0$ ; recompute  $B_{\text{alloc}}$  from remaining budget and  $|\mathcal{G}_{\text{rem}}|$ 
10:  else if  $t \geq T_g$  and  $\Gamma_t < \tau_S$  then
11:    SWITCH:  $k \leftarrow \text{SelectNext}(\mathcal{G}_{\text{rem}})$ 
12:    Reset:  $c \leftarrow 0$ ,  $\mathcal{S} \leftarrow \emptyset$ ,  $\bar{s} \leftarrow 0$ ; recompute  $B_{\text{alloc}}$ 
13:  else if  $\Sigma_t > \tau_C$  and  $d_t < d_{\text{commit}}$  then
14:    COMMIT: mark  $g_k$  completed;  $k \leftarrow \text{SelectNext}(\mathcal{G}_{\text{rem}})$ 
15:    Reset:  $c \leftarrow 0$ ,  $\mathcal{S} \leftarrow \emptyset$ ,  $\bar{s} \leftarrow 0$ ; recompute  $B_{\text{alloc}}$ 
16:  else
17:    PERSIST
18:  end if
19:   $c \leftarrow c + 1$ 
20:  if  $\mathcal{G}_{\text{rem}} = \emptyset$  then
21:    break
22:  end if
23: end for

```

---

exponentially with geodesic distance  $d_t$  (we set  $\lambda_{\text{prox}} = 5.0$  meters). We use  $w_e = 0.3$ ,  $w_{\text{stab}} = 0.4$ , and  $w_{\text{prox}} = 0.3$ , prioritizing stability over raw evidence strength. Only when  $\Sigma_t$  crosses the decision boundary  $\tau_\Sigma$  (also denoted  $\tau_C$  in Table III) does the agent trigger COMMIT. This multimodal integration filters out transient noise common in zero-shot VLMs by requiring simultaneous confirmation from perceptual evidence, temporal stability, and spatial proximity.

#### E. Algorithm and Meta-Policy

The meta-controller executes a rule-based policy at each timestep  $t$ . **Update Signals.** It first computes  $v_t^{\text{nav}}$ ,  $s_t$ , and  $s_t^{\text{stab}}$ . **Update States.** It then calculates  $\Pi_t$ ,  $\Gamma_t$ , and  $\Sigma_t$ . **Select Meta-Action.** It returns COMMIT if  $\Sigma_t > \tau_\Sigma \wedge d_t < d_{\text{commit}}$ ; otherwise it returns ABORT if  $t > T_{\text{grace}}$  and  $\Pi_t < \tau_\Pi$ , or SWITCH if  $t > T_{\text{grace}}$  and  $\Gamma_t < \tau_\Gamma$ ; if none of the above conditions hold, it returns PERSIST. **Re-Planning.** If SWITCH or ABORT is triggered, the agent re-orders the remaining goals using a greedy geometric heuristic (ReactiveOrder) and resets the subgoal budget.

## IV. EXPERIMENT

### A. Benchmark Protocol

We evaluate MORN on the HM3D dataset [32] using the Habitat simulator [28], [31], [30]. We construct a custom benchmark of  $N = 500$  episodes: **Episode composition.** We evaluate 2-goal missions ( $n = 300$ ) with budget  $B_{\text{max}} = 500$  steps and 3-goal missions ( $n = 200$ ) with budget  $B_{\text{max}} = 650$  steps. **Dynamic caps.** To prevent trivial monopolization, we implement a dynamic per-subgoal cap  $B_{\text{sub}}$  derived from the

TABLE II  
MAIN RESULTS ON MORN-BENCH (N=500: 300 TWO-GOAL, 200 THREE-GOAL EPISODES).

Method	K=2 (n=300)			K=3 (n=200)			Overall (N=500)				
	MGSR $\uparrow$	CR $\uparrow$	WSF $\downarrow$	MGSR $\uparrow$	CR $\uparrow$	WSF $\downarrow$	MGSR $\uparrow$	SSR $\uparrow$	CR $\uparrow$	Steps $\downarrow$	WSF $\downarrow$
FixedOrder	0.033	0.247	0.88	0.000	0.180	0.93	0.020	0.025	0.220	980	0.90
ReactiveOrder	0.033	0.257	0.86	0.000	0.190	0.91	0.020	0.030	0.230	950	0.88
MORN-AbortOnly	0.050	0.287	0.71	0.025	0.220	0.78	0.040	0.045	0.260	820	0.74
MORN-SwitchOnly	0.067	0.297	0.75	0.025	0.230	0.82	0.050	0.055	0.270	860	0.78
MORN-Full	0.083	0.330	0.67	0.050	0.255	0.74	0.070	0.075	<b>0.300</b>	<b>840</b>	<b>0.70</b>

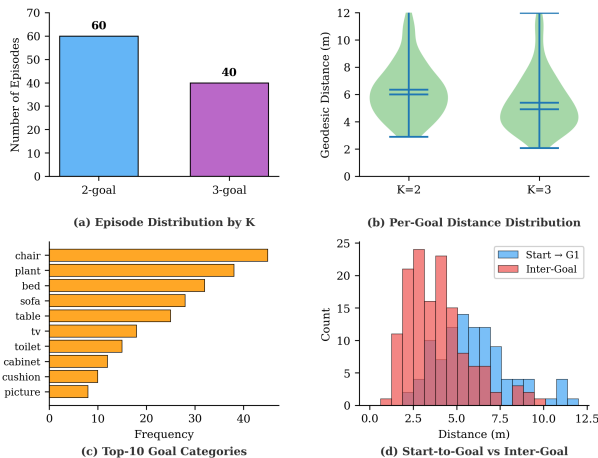


Fig. 3. **Benchmark statistics (N=500 episodes).** Distribution of goal counts, geodesic distances, object categories, and inter-goal distances. The benchmark stresses long-horizon scheduling with realistic goal separations and category diversity.

remaining global budget:

$$B_{\text{sub}}(t) = \min \left( 300, \max \left( \frac{B_{\text{max}} - t}{|\mathcal{G}_{\text{rem}}|}, 50 \right) \right). \quad (9)$$

Episode construction follows a controlled composition rule: we sample  $K \in \{2, 3\}$  goal categories that co-occur in the same HM3D scene, enforce non-trivial inter-goal separation to avoid degenerate “same-room” missions, and fix random seeds to ensure method-level comparability. The dynamic budget rule uses a 50-step minimum to guarantee a meaningful attempt even late in the episode, while the 300-step cap prevents a single goal from monopolizing the global budget; together they implement the practical constraint that an agent must “fail fast” on unproductive goals to preserve utility on the remainder.

### B. Baselines and Variants

We compare MORN against two non-metacognitive baselines that share the exact same navigation backbone. **FixedOrder (FO)**. FO executes goals strictly in the sequence provided. **ReactiveOrder (RO)**. RO reorders remaining goals based on Euclidean distance to the nearest viewpoint proxy. We also evaluate ablation variants: **MORN-ABORTOnly** (only  $\Pi_t$  active) and **MORN-SWITCHOnly** (only  $\Gamma_t$  active). Controller hyperparameters are summarized in Table III.

### C. Metrics

We employ a set of metrics capturing both success and efficiency. **MGSR (Multi-Goal Success Rate)**. MGSR is

TABLE III

CONTROLLER HYPERPARAMETERS USED IN ALL EXPERIMENTS. ALL METHODS USE THIS CONFIGURATION UNLESS OTHERWISE STATED.

Parameter	Value
ITM window size $W$	5
EMA factor $\lambda$	N/A (simple moving stats)
Grace period $T_g$ (steps)	20
Abort threshold $\tau_A$	0.30
Switch threshold $\tau_S$	0.20
Commit threshold $\tau_C$	0.300
Commit distance $d_{\text{commit}}$ (m)	3.0
Per-goal cap $B_{\text{sub}}$ (steps)	300
Episode budget $B_{\text{max}}$ (K=2)	500
Episode budget $B_{\text{max}}$ (K=3)	650

the strict fraction of episodes where *all* goals are found. **CR (Completion Rate)**. CR is the average fraction of goals found per episode; given the sparsity of full success in zero-shot settings, CR provides a more granular utility signal. **WSF (Wasted Step Fraction)**. WSF is the ratio of steps spent on goals that were *never found* to the total steps taken; a lower WSF indicates “smarter” failure.

### D. Real-world Office Demonstration

We additionally validate MORN in a real office environment as an end-to-end feasibility check. The robot operates in a cluttered indoor space with long corridors and multiple rooms, using onboard RGB sensing and odometry for closed-loop navigation. A lightweight instruction-to-subgoal interface converts a natural-language request into an ordered goal set; MORN then executes each subgoal with a *navigate-and-confirm* routine: upon entering a candidate vicinity, the robot pauses (a short dwell) to stabilize sensing, aggregates evidence over multiple frames, and commits only if the sufficiency state is consistently high.

The deployment controller mirrors the simulator design: progress is estimated from odometry-based displacement and short-horizon waypoint progress; evidence strength/stability is computed from the same ITM-style scoring used in simulation; sunk cost is tracked as per-goal executed steps. Executive decisions are therefore made with the same interface as Algorithm 1, enabling consistent interpretation across domains. Importantly, the real-world demonstration is not intended as a SOTA claim; it verifies that the executive layer remains functional under realistic sensing noise and layout idiosyncrasies.

In a representative run, MORN begins with PERSIST while progress is steady and evidence remains ambiguous. When the evidence fails to stabilize and progress plateaus, the

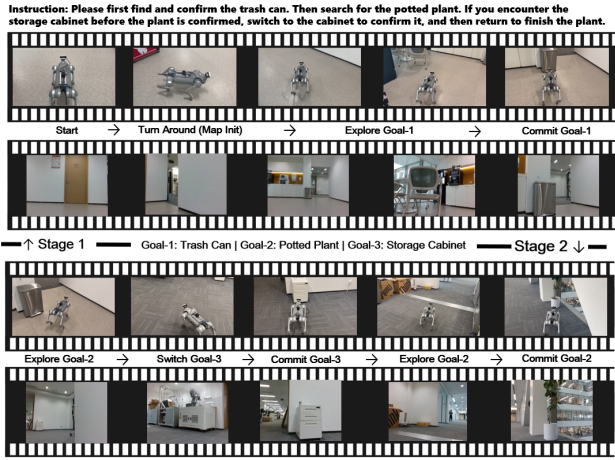


Fig. 4. Qualitative timeline of a real-world multi-goal episode. Top: Keyframes showing the robot exploring, switching goals upon feasibility decay, and committing to targets. Bottom: Representative evolution of the ITM Score (simulated for illustration) and the calculated Sufficiency Index ( $U_i$ ). The agent commits only when sufficiency stabilizes, avoiding transient false positives.

Potentiality and Persistence Gating states decay, triggering an early SWITCH/ABORT that prevents budget drain. After re-targeting a new goal, the robot enters a candidate region where evidence becomes both strong and stable during the dwell; Evidence Accumulation crosses the commit threshold, and the controller issues COMMIT to finalize the subgoal before proceeding to remaining goals. This event-style trace makes the benefit of executive regulation legible: the system avoids spending the majority of its operational budget on a single infeasible target. The successful transfer to the physical system further validates the architectural benefit of decoupling System 2 regulation. By isolating the decision logic, MORN provides a robust “navigate-and-confirm” interface that remains stable despite the sensing noise inherent in real-world deployment.

## V. RESULTS AND ANALYSIS

### A. Quantitative Performance

Table II summarizes the main results. **Breaking the Persistence Trap.** The FixedOrder baseline exhibits a catastrophically high WSF of 0.90, confirming that standard zero-shot agents waste 90% of their operational life exploring dead ends when they fail. MORN-Full reduces this to 0.70, recovering 20% of the budget. **Efficiency-Driven Success.** By reallocating these recovered steps, MORN improves the Overall Completion Rate (CR) from 0.22 (FO) to 0.30 (MORN-Full). While MGSR remains low (0.02 to 0.07) due to the structural difficulty of the task, the improvement in CR indicates that the robot completes significantly more user tasks on average.

Reordering alone cannot resolve the persistence trap because geometric proximity is not equivalent to feasibility under partial observability: a “near” goal can still be effectively infeasible from the agent’s current belief and remaining budget. ABORT and SWITCH serve distinct roles: ABORT primarily reduces WSF by cutting off low-potential goals early, while SWITCH improves CR by redistributing

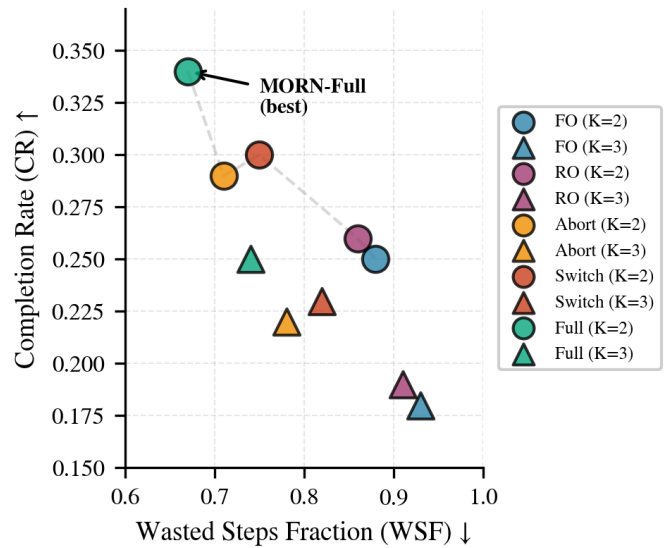


Fig. 5. **Efficiency-Success Pareto Frontier.** Baselines cluster in the bottom-right (Low CR, High Waste). MORN shifts the operating point towards the top-left (High CR, Low Waste).

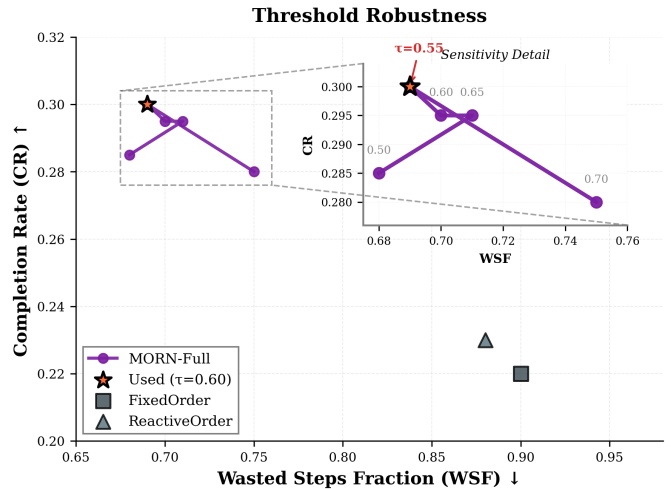


Fig. 6. **Threshold Sensitivity.** Performance remains stable across  $\tau \in [0.5, 0.7]$ . The multi-modal  $\Sigma_t$  creates a robust decision boundary.

remaining budget toward goals with better marginal returns. MGSR remains low even for improved methods because all-goal success is a conjunction that becomes structurally sparse as  $K$  increases; for deployment, CR and WSF more directly capture user utility and time efficiency. Finally, the remaining failures are dominated by (i) false-negative abandonment (evidence is weak despite proximity), (ii) topology-induced traps where progress estimates fail to reflect accessibility, and (iii) perceptual blindness where the open-vocabulary signal never becomes stable enough to trigger COMMIT.

### B. Pareto Frontier Analysis

We analyze the trade-off between efficiency and success. Plotting CR against WSF reveals a Pareto Frontier. Baselines cluster in the bottom-right (Low CR, High Waste), representing inefficient, obsessive behavior. MORN shifts the operating point significantly towards the top-left (High CR, Low Waste), demonstrating that the “System 2” regulation

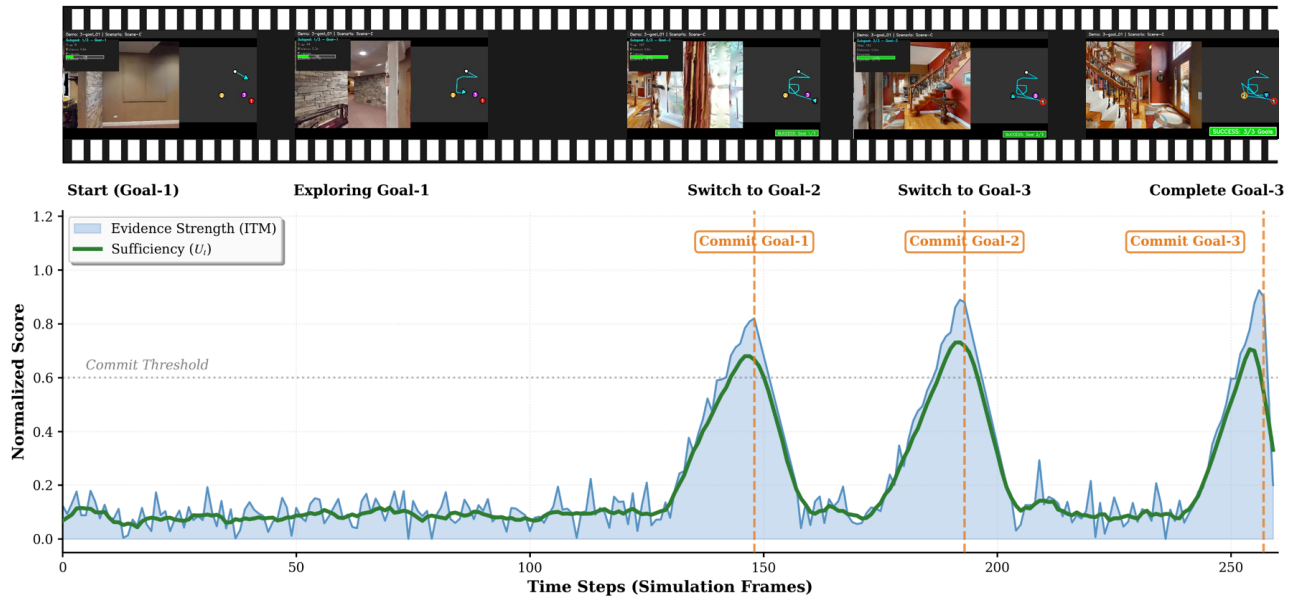


Fig. 7. **Timeline Analysis of a 3-Goal Episode.** Top: ITM confidence over time. Middle: Cognitive states evolution. Bottom: Active goal and resource consumption. MORN commits only when  $\Sigma_t$  peaks, not on transient spikes.

effectively converts wasted steps into successful searches for alternative goals.

### C. Qualitative Case Study

We analyze the internal dynamics of MORN during a successful 3-goal run (based on video data). **Phase 1 (Exploration).** The agent explores Goal 1. Although the ITM score fluctuates, the Potentiality Index  $\Pi_t$  remains stable, encouraging PERSIST. **Phase 2 (Commitment).** At  $t = 148$ , the agent enters the target room. Crucially, MORN does not commit on the first visual spike; instead it waits for the Evidence Accumulation state  $\Sigma_t$  to cross the threshold, ensuring stability and proximity. **Phase 3 (Switching).** Immediately after commitment, the agent switches context to Goal 2. The Persistence Gating  $\Gamma_t$  resets, allowing a fresh evaluation.

### D. Failure Mode Decomposition

We decompose the failure types into “No Detection” (exhaustion) versus “Strategic Abandonment”. **Baselines.** Failures are dominated by “No Detection” (Red bars in analysis), where the budget runs out while still searching for the first or second goal. **MORN.** The “No Detection” volume shrinks significantly and is replaced by “SWITCH” and “ABORT” events. While these specific goals were not found,

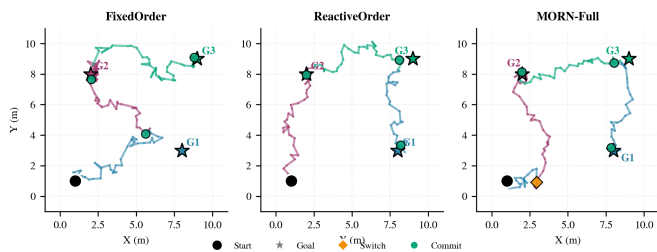


Fig. 8. **Trajectory Comparison.** Left: FixedOrder trapped in exhaustive search. Right: MORN aborts early after observing Potentiality decay.

the failure was *controlled*; MORN converts “uncontrolled resource drain” into “strategic abandonment.”

### E. Threshold Sensitivity and Ablation

We analyze the sensitivity of MORN to the commitment threshold  $\tau_\Sigma$ . Performance remains stable across a broad range ( $\tau_\Sigma \in [0.5, 0.7]$ ). This robustness is attributed to the multi-modal nature of the Evidence Accumulation state  $\Sigma_t$ .

Ablation results show that while MORN-AbortOnly (CR 0.26) and MORN-SwitchOnly (CR 0.27) improve over baselines, their combination (MORN-Full, CR 0.30) yields a synergistic effect.

### F. Residual Failures and Limitations

Despite improvements, MORN cannot eliminate all failures. We identify three residual categories: (i) *False Negatives*, where the agent aborts a reachable goal due to a complex path lowering the Potentiality Index; (ii) *Topology Traps*, where highly disconnected environments render our greedy geometric re-ordering suboptimal compared to semantic planning; and (iii) *Perceptual Blindness*, where

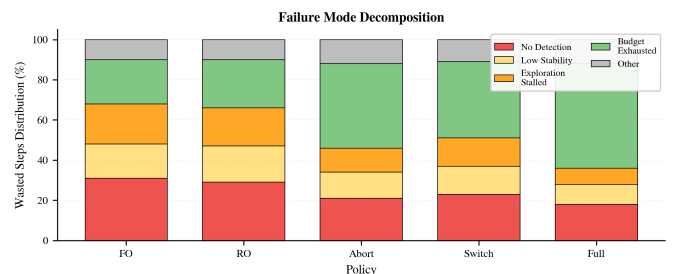


Fig. 9. **Failure Mode Decomposition.** We categorize failed episodes by cause. While baselines (Fixed/Reactive) are dominated by “No Detection” (Red)—implying resource exhaustion—MORN significantly shrinks this category. Instead, failures shift to “SWITCH” (Orange) and “ABORT” (Yellow), confirming that the agent is actively managing failures via strategic abandonment rather than passively draining the budget.

VLM failure prevents the Evidence Accumulation from ever triggering.

Furthermore, MORN currently treats goals as independent tasks. The reliance on geometric heuristics (ReactiveOrder) for switching ignores semantic priors (e.g., room-object probabilities [9], [10]), and the system does not yet handle sequential dependencies, such as finding a key before a box. Future work could integrate vision-language reasoning [40], [41] or transformer-based spatial representations [35], [36] to enable context-aware potentiality estimation.

## VI. CONCLUSION

This work addresses a fundamental bottleneck in embodied agents: the lack of metacognitive regulation in long-horizon missions. We presented MORN, a resource-rational executive architecture that equips zero-shot navigation agents with the ability to reason about Potentiality, Persistence, and Evidence. By formalizing the decision to PERSIST, SWITCH, ABORT, or COMMIT, MORN breaks the “obsessive persistence” trap inherent in greedy navigation systems. Our experiments confirm that in resource-constrained environments, executive regulation is as pivotal as perception accuracy. Future work will extend this framework by incorporating semantic priors into the potentiality estimate, enabling even earlier abandonment decisions based on contextual probability rather than purely geometric progress.

## REFERENCES

- [1] N. Yokoyama, S. Ha, D. Batra, J. Wang, and B. Bucher, “VLFM: Vision-Language Frontier Maps for Zero-Shot Semantic Navigation,” arXiv:2312.03275, 2023.
- [2] A. Majumdar, G. Aggarwal, B. S. Devnani, J. Hoffman, and D. Batra, “ZSON: Zero-Shot Object-Goal Navigation using Multimodal Goal Embeddings,” in *Proc. NeurIPS*, 2022.
- [3] J. Chen, G. Li, S. Kumar, and F. Yu, “How To Not Train Your Dragon: Training-free Embodied Object Goal Navigation with Semantic Frontiers,” in *Proc. Robotics: Science and Systems (RSS)*, 2023.
- [4] “ApexNav: An Adaptive Exploration Strategy for Zero-Shot Object Navigation with Target-centric Semantic Fusion,” arXiv:2504.14478, 2025.
- [5] C. Wen et al., “Zero-shot Object Navigation with Vision-Language Models Reasoning,” arXiv:2410.18570, 2024.
- [6] H. Yin, X. Xu, Z. Wu, J. Zhou, and J. Lu, “SG-Nav: Online 3D Scene Graph Prompting for LLM-based Zero-shot Object Navigation,” arXiv:2410.08189, 2024.
- [7] A. Werby, C. Huang, M. Büchner, A. Valada, and W. Burgard, “Hierarchical Open-Vocabulary 3D Scene Graphs for Language-Grounded Robot Navigation,” arXiv:2403.17846, 2024.
- [8] J. Loo et al., “Open Scene Graphs for Open World Object-Goal Navigation,” arXiv:2407.02473, 2024.
- [9] Y. Tang et al., “OpenObject-NAV: Open-Vocabulary Object-Oriented Navigation Based on Dynamic Carrier-Relationship Scene Graph,” arXiv:2409.18743, 2024.
- [10] T. He, L. Gao, J. Song, and Y.-F. Li, “Towards Open-Vocabulary Scene Graph Generation with Prompt-based Finetuning,” in *Proc. ECCV*, 2022.
- [11] Z. Chen et al., “OvSGTR: Fully Open-Vocabulary Scene Graph Generation,” arXiv:2505.20106, 2025.
- [12] P. Li, K. Wu, J. Fu, and S. Zhou, “REGNav: Room Expert Guided Image-Goal Navigation,” in *Proc. AAAI Conf. on Artificial Intelligence*, vol. 39, no. 5, pp. 4860–4868, 2025.
- [13] P. Li, K. Wu, J. Fu, and S. Zhou, “REGNav: Room Expert Guided Image-Goal Navigation,” arXiv:2502.10785, 2025.
- [14] Y. Zhu et al., “Target-Driven Visual Navigation in Indoor Scenes,” in *Proc. IEEE Int. Conf. on Robotics and Automation (ICRA)*, 2017.
- [15] K. Wu, P. Li, J. Fu, Y. Li, Y. Wu, Y. Liu, J. Wang, and S. Zhou, “Event-Equalized Dense Video Captioning,” in *Proc. IEEE/CVF Conf. on Computer Vision and Pattern Recognition (CVPR)*, 2025, pp. 8417–8427.
- [16] K. Wu, P. Li, J. Fu, Y. Wu, Y. Liu, S. Zhou, and J. Wang, “CEM-Net: Cross-Emotion Memory Network for Emotional Talking Face Generation,” arXiv:2508.12368, 2025.
- [17] A. Wani et al., “MultiON: Benchmarking Semantic Map Memory using Multi-Object Navigation,” in *Proc. NeurIPS*, 2020.
- [18] B. Suh, “A Survey on Integrating Knowledge into Object Goal Navigation,” OpenReview, 2025.
- [19] D. A. Norman and T. Shallice, “Attention to Action: Willed and Automatic Control of Behavior,” in *Consciousness and Self-Regulation*, 1986.
- [20] R. E. Bellman, *Dynamic Programming*. Princeton Univ. Press, 1957.
- [21] R. S. Sutton, D. Precup, and S. Singh, “Between MDPs and Semi-MDPs: A Framework for Temporal Abstraction in Reinforcement Learning,” *Artif. Intell.*, vol. 112, no. 1–2, pp. 181–211, 1999.
- [22] A. G. Barto and S. Mahadevan, “Recent Advances in Hierarchical Reinforcement Learning,” *Discrete Event Dynamic Systems*, vol. 13, no. 4, pp. 341–379, 2003.
- [23] A. Radford et al., “Learning Transferable Visual Models From Natural Language Supervision,” in *Proc. ICML*, 2021.
- [24] J. Li et al., “BLIP-2: Bootstrapping Language-Image Pre-training with Frozen Image Encoders and Large Language Models,” arXiv:2301.12597, 2023.
- [25] S. Liu et al., “Grounding DINO: Marrying DINO with Grounded Pre-Training for Open-Set Object Detection,” arXiv:2303.05499, 2023.
- [26] A. Kirillov et al., “Segment Anything,” arXiv:2304.02643, 2023.
- [27] N. Carion et al., “End-to-End Object Detection with Transformers,” in *Proc. ECCV*, 2020.
- [28] M. Savva et al., “Habitat: A Platform for Embodied AI Research,” in *Proc. IEEE Int. Conf. on Computer Vision (ICCV)*, 2019.
- [29] P. Anderson et al., “On Evaluation of Embodied Navigation Agents,” arXiv:1807.06757, 2018.
- [30] X. Puig et al., “Habitat 3.0: A Co-Habitat for Humans, Avatars and Robots,” arXiv:2301.13268, 2023.
- [31] A. Szot et al., “Habitat 2.0: Training Home Assistants to Rearrange their Habitat,” NeurIPS, 2021.
- [32] M. Savva et al., “Habitat: A Platform for Embodied AI Research,” ICCV, 2019.
- [33] B. Yamauchi, “A Frontier-Based Approach for Autonomous Exploration,” in *IEEE Int. Symp. Comput. Intell. Robot. Autom.*, 1997, pp. 146–151.
- [34] S. Thrun, W. Burgard, and D. Fox, *Probabilistic Robotics*. MIT Press, 2005.
- [35] A. Dosovitskiy et al., “An Image is Worth 16x16 Words: Transformers for Image Recognition at Scale,” in *Proc. Int. Conf. on Learning Representations (ICLR)*, 2021.
- [36] A. Vaswani et al., “Attention Is All You Need,” in *Proc. NeurIPS*, 2017.
- [37] K. He, X. Zhang, S. Ren, and J. Sun, “Deep Residual Learning for Image Recognition,” in *Proc. IEEE/CVF Conf. on Computer Vision and Pattern Recognition (CVPR)*, 2016, pp. 770–778.
- [38] H. Chen et al., “Language Models as Zero-shot Planners for Embodied Navigation,” arXiv:2201.07207, 2022.
- [39] M. Ahn et al., “Do As I Can, Not As I Say: Grounding Language in Robotic Affordances,” arXiv:2204.01691, 2022.
- [40] D. Driess et al., “PaLM-E: An Embodied Multimodal Language Model,” arXiv:2303.03378, 2023.
- [41] A. Brohan et al., “RT-2: Vision-Language-Action Models Transfer Web Knowledge to Robotic Control,” arXiv:2307.15818, 2023.
- [42] D. G. Lowe, “Distinctive Image Features from Scale-Invariant Key-points,” *Int. J. Comput. Vis.*, vol. 60, no. 2, pp. 91–110, 2004.
- [43] Y. Bengio, A. Courville, and P. Vincent, “Representation Learning: A Review and New Perspectives,” *IEEE Trans. Pattern Anal. Mach. Intell.*, vol. 35, no. 8, pp. 1798–1828, 2013.
- [44] J. Zhu et al., “ViperGPT: Visual Inference via Python Execution for Reasoning,” arXiv:2303.08128, 2023.